Post-print version:

Gain scheduling control of variable-speed wind energy conversion systems using quasi-LPV models

F.D. Bianchi, R. Mantz and C.F. Christiansen

This work has been published in **Control Engineering Practice**:

F.D. Bianchi, R. Mantz and C.F. Christiansen, "Gain scheduling control of variable-speed wind energy conversion systems using quasi-LPV models", *Control Engineering Practice*, vol. 13, no. 2, pp. 247-255, 2005.

Final version available at:

URL: http://www.sciencedirect.com/science/article/pii/S0967066104000541

DOI: 10.1016/j.conengprac.2004.03.006

© 2005. This manuscript version is made available under the CC-BY-NC-ND 4.0 license
http://creativecommons.org/licenses/by-nc-nd/4.0/

BibTex:

```
@Article{Bianchi2005,
    Title    = {Gain scheduling control of variable-speed wind energy conversion
       systems using quasi-LPV models},
    Author   = {Fernando D. Bianchi and Ricardo Mantz and Carlos Frede
       Christiansen},
    Journal  = {Control Engineering Practice},
    Year     = {2005},
    Number   = {2},
    Pages    = {247-255},
    Volume   = {13},
    Doi      = {10.1016/j.conengprac.2004.03.006}
}
```

Gain scheduling control of variable-speed wind energy conversion systems using quasi-LPV models.

F.D.Bianchi [1,*] R.J.Mantz [2] C.F.Christiansen [3]

Laboratorio de Electrónica Industrial, Control e Instrumentación (LEICI), Facultad de Ingeniería, Universidad Nacional de La Plata, CC 91, 1900 La Plata, Argentina

Abstract

The paper deals with the control of variable-speed wind energy conversion systems (WECS) in the context of linear parameter varying (LPV) systems, a recent formulation of the classic gain scheduling technique. The LPV approach is specially useful in variable-speed WECS control, which is characterized by nonlinear dynamic behavior and opposite objectives. In particular, the following objectives are considered: conversion efficiency maximization, safe operation, resonant modes damping, and robust stability. The proposed LPV controller is compared with a fixed controller that also takes into account the nonlinear behavior of the wind turbine.

Key words:
Linear parameter varying systems, gain scheduling, wind energy conversion system, wind turbines

1 Introduction

Nowadays, variable-speed wind energy conversion systems (WECS) are receiving considerable interest because they are able to maximize the energy capture and to reduce the aerodynamic load for a wide range of wind speeds. In variable-speed WECS, an electronic converter uncouples the rotational

* Corresponding author. Phone/Fax: +54 221 4259306.
Email address: fbianchi@ing.unlp.edu.ar (F.D.Bianchi).
[1] CONICET - UNLP
[2] CICpBA - UNLP
[3] UNLP

speed from the grid frequency, allowing the wind turbine to work at optimal operating conditions at different wind speeds (**???**). Also, it is known that WECS present nonlinear dynamic behavior and lightly damped resonant modes. When the frequency range of the disturbances matches one of the resonant modes, the life of the turbine components is reduced, and the generated power quality is deteriorated (**??**). Typical objectives are: to maximize energy capture in low wind speed, to maintain the generated power and the rotational turbine speed within safe limits during high wind speeds, and to avoid lightly damped resonant modes in the closed loop system (**??**).

On the other hand, control techniques based on gain scheduling concepts are extensively used in practical applications. The classic gain scheduling approach consists in designing linear controllers for several operating points and then applying an interpolation strategy to obtain a global control. Consequently, powerful tools for linear systems can be applied to nonlinear plants. In spite of the numerous applications, there was not a formal framework until the beginning of the nineties (**??**). This framework gives heuristic rules to ensure global stability, but it does not provide a systematic design procedure. Later, **?** introduce the linear parameter varying (LPV) systems. In this context, the synthesis problem can be formulated as a convex optimization problem with linear matrix inequality (LMI) constraints wherein the controller is considered as a simple entity without the classical interpolations drawbacks (**????**).

This paper deals with the modelling and control of variable-speed WECS using the LPV gain scheduling approach. Analogously to linear optimal control, it is possible to design a controller that considers the nonlinear nature of wind turbines, aims to balance opposed objectives, and ensures stability with model uncertainty.

This paper is structured as follows, Section 2 presents a brief summary of LPV gain scheduling techniques. In Section 3 the dynamic equations of WECS are deduced. Then, in Section 4, the problem specifications are discussed. Finally, the proposed LPV gain scheduling controller is presented in Section 5.

2 LPV Gain Scheduling

Linear parameter varying (LPV) systems can be considered as a particular case of linear time varying (LTV) systems where the matrices of the state model are continuous and fixed functions of some varying parameter vector $\theta(t) \in \mathbb{R}^s$. That is

$$\dot{\mathbf{x}}(t) = \mathbf{A}(\theta(t))\mathbf{x}(t) + \mathbf{B}(\theta(t))\mathbf{w}(t), \tag{1}$$

$$\mathbf{z}(t) = \mathbf{C}(\theta(t))\mathbf{x}(t) + \mathbf{D}(\theta(t))\mathbf{w}(t)$$

where $\mathbf{x}$ is the state ($\mathbf{x} \in \mathbb{R}^n$), $\mathbf{w}$ is the input, and $\mathbf{z}$ is the output. The parameter vector $\theta(t)$ is not known *a priori*, but it is assumed in a bounded set $\Theta \subset \mathbb{R}^s$.

If there exits a symmetric positive definite matrix $\mathbf{P} \in \mathbb{R}^{n \times n}$ such that

$$\begin{bmatrix} \mathbf{A}(\theta)^T\mathbf{P} + \mathbf{P}\mathbf{A}(\theta) & \mathbf{P}\mathbf{B}(\theta) & \mathbf{C}(\theta)^T \\ \mathbf{B}(\theta)^T\mathbf{P} & -\gamma\mathbf{I} & \mathbf{D}(\theta)^T \\ \mathbf{C}(\theta) & \mathbf{D}(\theta) & -\gamma\mathbf{I} \end{bmatrix} < 0 \tag{2}$$

for any possible trajectory $\theta(t)$, the system (1) is exponentially stable, and it can be assured that $\|\mathbf{z}\|_2 \leq \gamma\|\mathbf{w}\|_2 \; \forall\theta(t) \in \Theta$ and $\gamma > 0, \gamma \in \mathbb{R}$ (**??**).

Given the open loop system

$$\begin{aligned} \dot{\mathbf{x}}(t) &= \mathbf{A}(\theta(t))\mathbf{x}(t) + \mathbf{B}_1(\theta(t))\mathbf{w}(t) + \mathbf{B}_2(\theta(t))\mathbf{u}(t), \\ \mathbf{z}(t) &= \mathbf{C}_1(\theta(t))\mathbf{x}(t) + \mathbf{D}_{11}(\theta(t))\mathbf{w}(t) + \mathbf{D}_{12}(\theta(t))\mathbf{u}(t), \\ \mathbf{y}(t) &= \mathbf{C}_2(\theta(t))\mathbf{x}(t) + \mathbf{D}_{21}(\theta(t))\mathbf{w}(t), \end{aligned} \tag{3}$$

with the control input $\mathbf{u}$ and the measured output $\mathbf{y}$, the LPV gain scheduling synthesis problem consists in finding a controller

$$\begin{aligned} \dot{\mathbf{x}}_k(t) &= \mathbf{A}_k(\theta(t))\mathbf{x}_k(t) + \mathbf{B}_k(\theta(t))\mathbf{y}(t), \\ \mathbf{u}(t) &= \mathbf{C}_k(\theta(t))\mathbf{x}_k(t) + \mathbf{D}_k(\theta(t))\mathbf{y}(t) \end{aligned} \tag{4}$$

such that the closed loop system satisfies (2). Notice that although the parameter vector $\theta(t)$ must be measured in real-time, for the controller design only the bounded set Θ is required.

This synthesis problem can be formulated as a convex optimization problem with LMI constraints (**????**). Hence, a complete and systematic solution using the efficient interior point algorithms is achieved (**?**). In this context, **?** present the basic characterization to incorporate into the synthesis problem multiple specifications such as $\mathcal{H}_2/\mathcal{H}_\infty$ constraints and pole clustering. In the same work, the authors consider parameter-dependent scalings to exploit the structural information on the operator $\mathbf{w} \to \mathbf{z}$.

The mathematical formulation required to synthesize the proposed controller is summarized as follows. The plant (3) is considered with $\mathbf{w}$ and $\mathbf{z}$ subject to

$$[\mathbf{w}_1(t), \ldots, \mathbf{w}_m(t)]^T = \mathbf{\Delta}(t)[\mathbf{z}_1(t), \ldots, \mathbf{z}_m(t)]^T$$

where the operator $\Delta(t)$ has the following structure

$$\mathbf{\Delta} := \text{diag}(\mathbf{\Delta}_1(t), ..., \mathbf{\Delta}_m(t)), \quad \text{with} \quad \sigma_{max}(\mathbf{\Delta}(t)) \leq 1/\gamma, \quad \forall t \geq 0.$$

Also, the following associated set of parameter-dependent scalings is defined

$$\mathcal{S}_{\mathbf{\Delta}} := \{\mathbf{S} : \mathbf{S} > 0, \mathbf{S}\mathbf{\Delta}(t) = \mathbf{\Delta}(t)\mathbf{S}, \ \forall t \geq 0\}.$$

Assuming that the parameter dependence of the plant (3) is affine , $\mathbf{B}_2$, $\mathbf{C}_2$, $\mathbf{D}_{12}$, $\mathbf{D}_{21}$ are constant and Θ is a polytope with vertices θ_i, then, the controller can be obtained by solving the following set of LMIs

$$\begin{bmatrix} \mathbf{X}\mathbf{A}_i + \hat{\mathbf{B}}_{k_i}\mathbf{C}_2 + (\star) & \star & \star & \star \\ \hat{\mathbf{A}}_{k_i}^T + \mathbf{A}_i + \mathbf{B}_2\mathbf{D}_{k_i}\mathbf{C}_2 & \mathbf{A}_i\mathbf{Y} + \mathbf{B}_2\hat{\mathbf{C}}_{k_i} + (\star) & \star & \star \\ \mathbf{S}_i^{-1}(\mathbf{X}\mathbf{B}_{1_i} + \hat{\mathbf{B}}_{k_i}\mathbf{D}_{21})^T & \mathbf{S}_i^{-1}(\mathbf{B}_{1_i} + \mathbf{B}_2\mathbf{D}_{k_i}\mathbf{D}_{21})^T & -\gamma\mathbf{S}_i^{-1} & \star \\ \mathbf{C}_{1_i} + \mathbf{D}_{12}\mathbf{D}_{k_i}\mathbf{C}_2 & \mathbf{C}_{1_i}\mathbf{Y} + \mathbf{D}_{12}\hat{\mathbf{C}}_{k_i} & (\mathbf{D}_{11} + \mathbf{D}_{12}\mathbf{D}_{k_i}\mathbf{D}_{21})\mathbf{S}_i^{-1} & -\gamma\mathbf{S}_i^{-1} \end{bmatrix} < 0, \quad (5)$$

$$\begin{bmatrix} \mathbf{X} & \mathbf{I} \\ \mathbf{I} & \mathbf{Y} \end{bmatrix} > 0 \quad (6)$$

where $\mathbf{X}$, $\mathbf{Y}$, $\hat{\mathbf{A}}_{k_i}$, $\hat{\mathbf{B}}_{k_i}$, $\hat{\mathbf{C}}_{k_i}$, $\mathbf{D}_{k_i}$ and $\mathbf{S}_i$ are the decision variables, and the terms denoted $\star$ are induced by symmetry. Finally, the controller matrices are computed with the following expressions

$$\mathbf{A}_{k_i} = \mathbf{N}^{-1}(\hat{\mathbf{A}}_{k_i} - \mathbf{X}(\mathbf{A}_i - \mathbf{B}_2\mathbf{D}_{k_i}\mathbf{C}_2)\mathbf{Y} - \hat{\mathbf{B}}_{k_i}\mathbf{C}_2\mathbf{Y} - \mathbf{X}\mathbf{B}_2\hat{\mathbf{C}}_{k_i})\mathbf{M}^{-T}, \quad (7)$$

$$\mathbf{B}_{k_i} = \mathbf{N}^{-1}(\hat{\mathbf{B}}_{k_i} - \mathbf{X}\mathbf{B}_2\mathbf{D}_{k_i}), \quad (8)$$

$$\mathbf{C}_{k_i} = (\hat{\mathbf{C}}_{k_i} - \mathbf{D}_{k_i}\mathbf{C}_2\mathbf{Y})\mathbf{M}^{-T} \quad (9)$$

where $\mathbf{M}$ and $\mathbf{N}$ are obtained from solving $\mathbf{I} - \mathbf{X}\mathbf{Y} = \mathbf{N}\mathbf{M}^T$.

Note that the synthesis problem with the scaling $\mathbf{S}(\theta(t))$ is not convex. Nevertheless, a computational procedure similar to the D-K iterations of μ-synthesis can be applied (**?**).

Moreover, the resulting controllers may present unnecessarily fast modes (**?**), that would complicate the implementation. To circumvent this problem, the location of the closed loop poles of the underlying LTI system (at fixed θ) is forced to lie in certain region $\mathcal{D} \in \mathbb{C}$ by complementing the set of LMIs (5)-(6) with

$$\begin{bmatrix} \lambda_{jk} \begin{bmatrix} \mathbf{Y} & \mathbf{I} \\ \mathbf{I} & \mathbf{X} \end{bmatrix} + \mu_{jk} \begin{bmatrix} \mathbf{A}_i\mathbf{Y} + \mathbf{B}_2\hat{\mathbf{C}}_{k_i} & \mathbf{A}_i + \mathbf{B}_2\mathbf{D}_{k_i}\mathbf{C}_2 \\ \hat{\mathbf{A}}_{k_i} & \mathbf{X}\mathbf{A}_i + \hat{\mathbf{B}}_{k_i}\mathbf{C}_2 \end{bmatrix} + \end{bmatrix}$$

$$+ \mu_{kj} \begin{bmatrix} \mathbf{A}_i\mathbf{Y} + \mathbf{B}_2\hat{\mathbf{C}}_{k_i} & \mathbf{A}_i + \mathbf{B}_2\mathbf{D}_{k_i}\mathbf{C}_2 \\ \hat{\mathbf{A}}_{k_i} & \mathbf{X}\mathbf{A}_i + \hat{\mathbf{B}}_{k_i}\mathbf{C}_2 \end{bmatrix}^T \Bigg]_{j,k} < 0 \qquad (10)$$

where λ_{jk} and μ_{jk} define the geometry of the region $\mathcal{D}$ (**?**).

3 System Description

3.1 Wind Turbine

For a wind turbine of radius R, the generated power and the mechanical torque have the following expressions, respectively

$$P_a = \frac{1}{2}\rho\pi R^2 C_p(\lambda) V^3, \qquad (11)$$

$$Q_a = \frac{1}{2}\rho\pi R^3 C_q(\lambda) V^2 \qquad (12)$$

where

V : wind speed,

λ : tip-speed ratio defined as $R\omega/V$,

ρ : air density,

ω : rotational speed of the wind turbine,

$C_p(\lambda)$: power coefficient defined as the ratio between the power captured by the wind turbine and the available wind power, that is the turbine efficiency to convert the kinetic energy of the wind into mechanical energy,

$C_q(\lambda)$: torque coefficient ($C_q(\lambda) = C_p(\lambda)/\lambda$).

The coefficient $C_p(\lambda)$ presents a maximum at $\lambda = \lambda_{opt}$ corresponding to maximum power generation.

Fig. 1 shows the aerodynamic torque as function of the rotational speed for several wind speeds (solid line) and the locus of maximum power generation corresponding to $\lambda = \lambda_{opt}$ (dotted line).

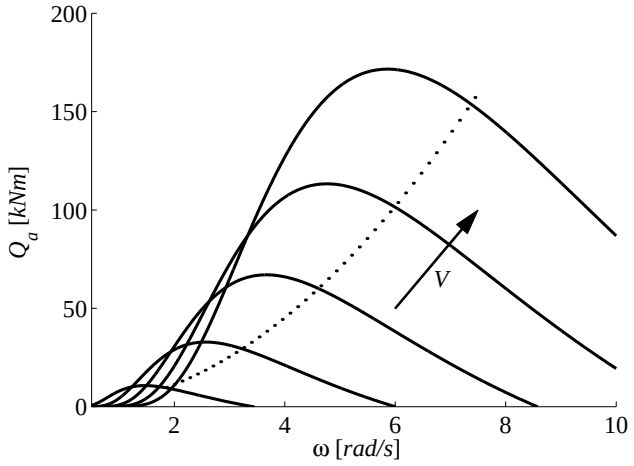

Figure 1. Aerodynamic torque for several wind speeds (solid line), and locus of maximum power generation corresponding to $\lambda = \lambda_{opt}$ (dotted line).

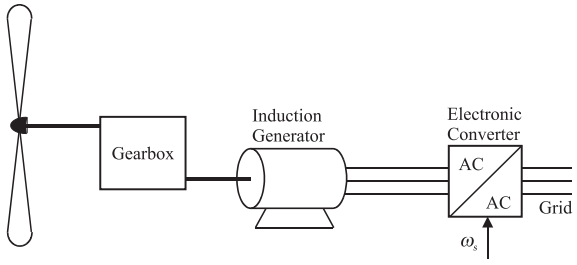

Figure 2. Variable-speed wind energy conversion system (WECS).

3.2 Dynamic model of the WECS

The WECS considered in this paper consist of a wind turbine, an induction generator and an electronic converter (Fig. 2). The electronic converter controls the generator torque so that the operating point can be set according to the generation strategy. The gearbox adapts the rotational speeds of the wind turbine and the electric generator. The system is connected to a stiff grid that can absorb all power supplied by the wind turbine without considerable change neither in voltage nor in frequency.

Usually, WECS are modelled as a series of inertias linked by flexible shafts with friction (**??**). Nevertheless, it must be stressed that wind turbines are flexible systems and, when are modelled through concentrated parameters, the elements of the model do not necessarily have direct correspondence with the physical elements of the system.

A model with a single dominant resonant mode is considered (Fig. 3). Then, the WECS dynamics equations are

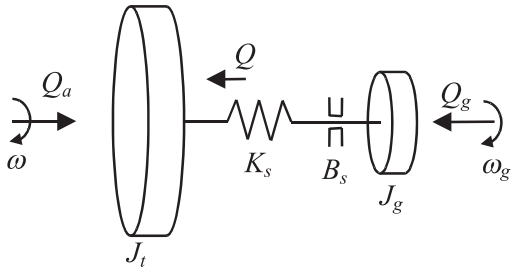

Figure 3. Mechanical model of the WECS.

$$J_t\dot{\omega} = Q_a - Q, \tag{13}$$
$$J_g\dot{\omega}_g = Q - Q_g, \tag{14}$$
$$\dot{Q} = K_s(\omega - \omega_g) + B_s(\dot{\omega} - \dot{\omega_g}) \tag{15}$$

where J_t and J_g are the moments of inertia of the wind turbine and the generator respectively, K_s is the stiffness coefficient, B_s is the friction coefficient, and ω_g is the generator shaft speed (all parameters are referred to the turbine side). Note that the equations (13)-(15) are not linear due to the highly nonlinear expression of Q_a (12).

Under the reasonable assumption that the mechanical dynamics is dominant compared with the electric one, the steady state model of the generator is adequate for torque calculation. Moreover, since the slip is small, the generator torque Q_g can be considered linear in ω_g:

$$Q_g = Q_{g1}\omega_g + Q_{g2}\omega_s \tag{16}$$

where

$$Q_{g1} = \frac{3}{R_r}\left[\frac{V_f \cdot n}{\omega_s}\right]^2, \quad Q_{g2} = \frac{3n}{R_r}\left[\frac{V_f}{\omega_s}\right]^2, \quad \omega_s = \frac{2\pi f}{p},$$

R_r is the rotor resistance, V_f is the stator voltage, n is the gearbox ratio which is assumed ideal (constant and without dynamics), f is the frequency and p is the number of pairs of poles.

3.3 Cyclic disturbances

Due to the non-uniformity of the wind speed in the area swept by the wind turbine, the aerodynamic torque presents oscillatory components known as cyclic disturbances. There are several causes of these wind speed variations such as: wind shear caused by wind speed variations over the rotor height, tower shadow caused by the support structure interfering with the air flow,

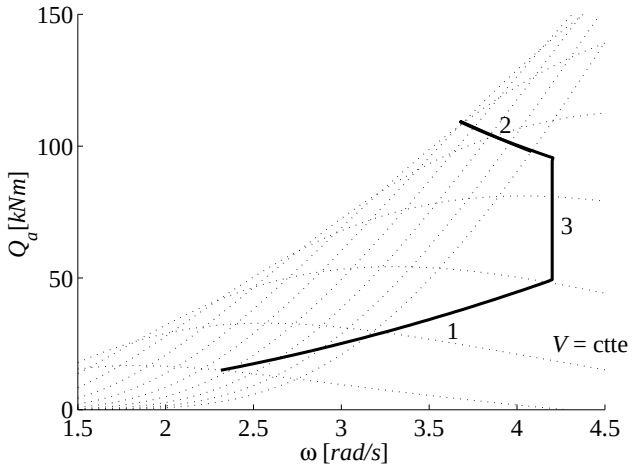

Figure 4. Set of operating points for a variable-speed WECS, superimposed to the aerodynamic torque for several wind speeds. 1-constant λ_{opt} region, 2-constant power region, and 3-constant ω region.

and yaw misalignment caused by the alignment error between the turbine shaft and the wind speed direction. In all cases, the cyclic disturbances, for a wind turbine of N blades, can be modelled as oscillatory components of the wind speed with harmonics in multiples of $N\omega$ (**?**).

4 Control objectives

Commonly, the control objectives for a variable-speed WECS are (**??**):

- To maintain the turbine in a set of operating points depending on the wind speed (**??**). At low speeds, λ must be maintained at its optimal value to maximize the conversion efficiency. On the other hand, at high wind speeds, the generated power should not exceed the nominal power. Additionally, to prevent large torque and power peaks, the turbine speed has to be maintained at constant speed between low and high wind speed regions. Fig. 4 shows a typical set of operating points according to the three mentioned regions. Usually, this objective is achieved by reference tracking. In this work it is adopted a speed reference ω_{ref} computed from the wind speed (**???**).
- To avoid lightly damped resonant modes in the closed system that can be excited by cyclic disturbances or wind turbulence. In this situation, the torque oscillation are incremented, and hence the useful life of the wind turbine may be reduced. Moreover, several components may suffer considerable damage. The problem is made worse in variable speed WECS because the harmonic components change with the turbine speed.

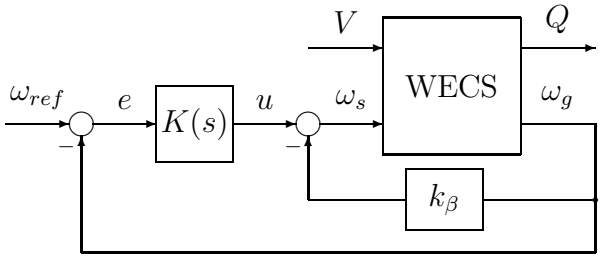

Figure 5. Block diagram for damping increment strategy.

Optimization techniques can provide a trade-off between the aforementioned objectives. However, the second requirement is not easy to fulfill. An indirect way, proposed by **?**, consists in modifying the slope of the incremental generator torque characteristic. Indeed, if a feedback gain k_β is used as in Fig. 5 where

$$k_\beta = \frac{Q_{g1} - \beta}{Q_{g2}}, \tag{17}$$

then the generator torque results

$$Q_g = \beta\omega_g + Q_{g2}u. \tag{18}$$

Fig. 6 shows the frequency response of the transfers $V \to Q$ and $\omega_{ref} \to e$ ($e = \omega_{ref} - \omega_g$) corresponding to the linearized system at one operating point for several values of k_β and $K = 1/s$. It can be observed that there exists one value of k_β in which the damping is maximum whereas for smaller and larger values of k_β the transfer $V \to Q$ presents resonant peaks.

Despite their outstanding contributions, this strategy does not guarantee robustness. Effectively, stability and performance are only assured at the design operating point and for a good model. Unfortunately, due to the complexity of WECS is very difficult to have an exact model, specially at high frequencies.

5 LPV Gain-scheduling strategy

5.1 Quasi-LPV model of the WESC

The model given by the equations (13)-(15) can be expressed as

$$\dot{\mathbf{x}} = \mathbf{A}\mathbf{x} + \mathbf{B}\mathbf{u} + \mathbf{f}(x_1, V) \tag{19}$$

where

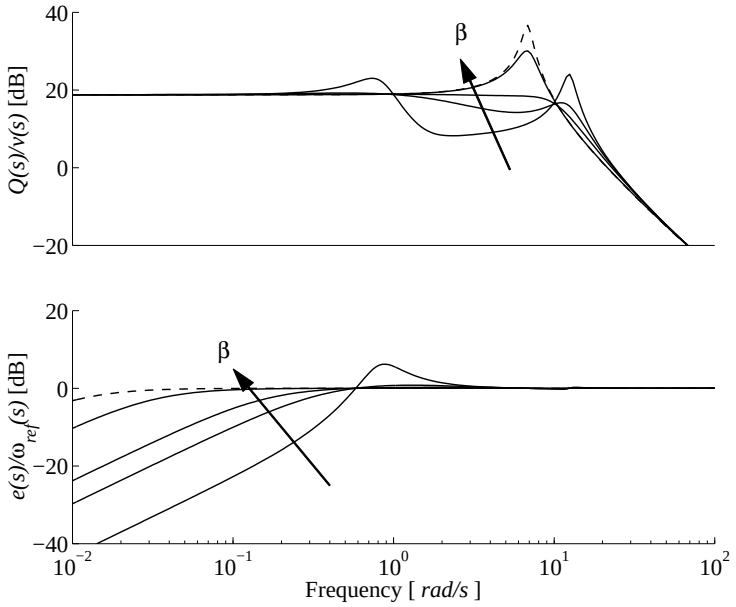

Figure 6. 1-Transfer $V \to Q$, 2-transfer $\omega_{ref} \to e$ corresponding to the block diagram in Fig. 5 for several values of β and $K = 1/s$. The $k_\beta = Q_{g1}$ transfers is indicated with dashed line.

$$\mathbf{A} = \begin{bmatrix} 0 & 0 & -1/J_t \\ 0 & -Q_{g1}/J_g & 1/J_g \\ K_s & (B_s Q_{g1}/J_g - K_s) & -B_s(1/J_t + 1/J_g) \end{bmatrix},$$

$$\mathbf{B}^T = \begin{bmatrix} 0 & -Q_{g2}/J_g & B_s Q_{g2}/J_g \end{bmatrix},$$

$$\mathbf{f}^T(x_1, V) = \begin{bmatrix} Q_a(x_1, V)/J_t & 0 & B_s Q_a(x_1, V)/J_t \end{bmatrix}.$$

Then, if there exist three differentiable functions (x_{2e}, x_{3e}, u_e) such that

$$\mathbf{A} \begin{bmatrix} x_1 \\ x_{2e} \\ x_{3e} \end{bmatrix} + \mathbf{B} u_e + \mathbf{f}(x_1, V) = 0, \tag{20}$$

by applying the states transformations proposed by **?** the WECS can be represented as a LPV model. Certainly, with these three functions, the states and the control inputs are redefined in the following way.

$$\xi_1 = x_1 = \omega, \tag{21}$$

$$\xi_2 = x_2 - x_{2e} = \omega_g - \omega, \tag{22}$$

$$\xi_3 = x_3 - x_{3e} = Q - Q_a(x_1, V), \tag{23}$$

$$\mu = u - u_e = \omega_s - (Q_a(x_1, V) - Q_{g1}x_1)/Q_{g2}. \tag{24}$$

Unfortunately, exact measurements of both x_1 and V are not possible. Actually, the turbine speed is an inaccessible variable, and it must be estimated from ω_g. On the other hand, the measured wind speed V is an average variable without information on cyclic disturbances [4]. Consequently, the bias term u_e ($u_e(\omega, V) = (Q_a(x_1, V) - Q_{g1}x_1)/Q_{g2}$) can not be correctly computed, and the performance will be deteriorated since the resultant error is a disturbance at the control input.

Clearly, this problem disappears if the bias term u_e is removed from (24). To this end, consider the nonlinear system (13)-(15) with an integral action at the input ω_s. Now, the states and matrices in (19) are

$$\mathbf{x}^T = \begin{bmatrix} \omega & \omega_g & Q & \omega_s \end{bmatrix},$$

$$\mathbf{A} = \begin{bmatrix} 0 & 0 & -1/J_t & 0 \\ 0 & -Q_{g1}/J_g & 1/J_g & Q_{g2}/J_g \\ K_s & (B_sQ_{g1}/J_g - K_s) & -B_s(1/J_t + 1/J_g) & B_sQ_{g2}/J_g \\ 0 & 0 & 0 & 0 \end{bmatrix},$$

$$\mathbf{B}^T = \begin{bmatrix} 0 & 0 & 0 & 1 \end{bmatrix},$$

$$\mathbf{f}(x_1, V)^T = \begin{bmatrix} Q_a(x_1, V)/J_t & 0 & B_sQ_a(x_1, V)/J_t & 0 \end{bmatrix}.$$

Then, applying the previous transformation, the new states result

$$\xi_1 = x_1 = \omega, \tag{25}$$
$$\xi_2 = x_2 - x_{2e} = \omega_g - \omega, \tag{26}$$
$$\xi_3 = x_3 - x_{3e} = Q - Q_a, \tag{27}$$
$$\xi_4 = x_4 - x_{4e} = \omega_s - (Q_a - Q_{g1}x_1)/Q_{g2}. \tag{28}$$

where the control input is the integrator input and the bias term u_e effectively becomes zero.

Finally, the quasi-LPV model is

[4] The cyclic disturbances are modeled as a wind component; however, they are actually caused by the turbine itself.

$$\dot{\xi} = \hat{\mathbf{A}}(\theta)\,\xi + \hat{\mathbf{B}}(\theta)\begin{bmatrix}\dot{V}\\ \mu\end{bmatrix}, \tag{29}$$

$$\mathbf{z} = \hat{\mathbf{C}}_1\,\xi,$$
$$\mathbf{y} = \hat{\mathbf{C}}_2\,\xi,$$

with

$$\theta = \begin{bmatrix}\omega_g & V\end{bmatrix}^T,$$

$$\hat{\mathbf{A}} = \begin{bmatrix} 0 & 0 & -1/J_t & 0 \\ 0 & -Q_{g1}/J_g & (1/J_g + 1/J_t) & -Q_{g1}/J_g \\ 0 & (B_s Q_{q1}/J_g - K_s) & (-B_s(1/J_g + 1/J_t) + 2q_2\theta_1/J_t + q_1\theta_2/J_t) & B_s Q_{g2}/J_g \\ 0 & 0 & (2q_2\theta_1 + q_1\theta_2 - Q_{g1})/Q_{g2}J_t & 0 \end{bmatrix},$$

$$\hat{\mathbf{B}} = \begin{bmatrix} 0 & 0 \\ 0 & 0 \\ -q_1\theta_1 - 2q_0\theta_2 & 0 \\ (-q_1\theta_1 - 2q_0\theta_2)/Q_{g2} & 1 \end{bmatrix},$$

$$\hat{\mathbf{C}}_1 = \begin{bmatrix} 0 & (-K_s + B_s Q_{g1}/J_g) & -B_s(1/J_g + 1/J_t) & B_s Q_{g2}/J_g \end{bmatrix},$$

$$\hat{\mathbf{C}}_2 = \begin{bmatrix} 1 & 1 & 0 & 0 \end{bmatrix},$$

where the aerodynamic torque is considered as

$$Q_a = q_2\omega^2 + q_1\omega V + q_0 V^2. \tag{30}$$

The coefficients q_2, q_1, and q_0 come from the following polynomial approximation

$$C_q = c_2\lambda^2 + c_1\lambda + c_0. \tag{31}$$

Note that the functions x_{2e}, x_{3e}, and x_{4e}, which satisfy (20), correspond to the equilibrium points expressed as functions of the state x_1 and the external signal V. That is, the new states represent deviations with respect to the equilibrium points. However, this is not a classical linearization, and the equation (29) exactly represents the nonlinear system (19). In this situation, where some of the parameter are states, the model is named as quasi-LPV. Also, it can be observed that the wind speed derivative in (29) is not a problem because it can be considered as a disturbance.

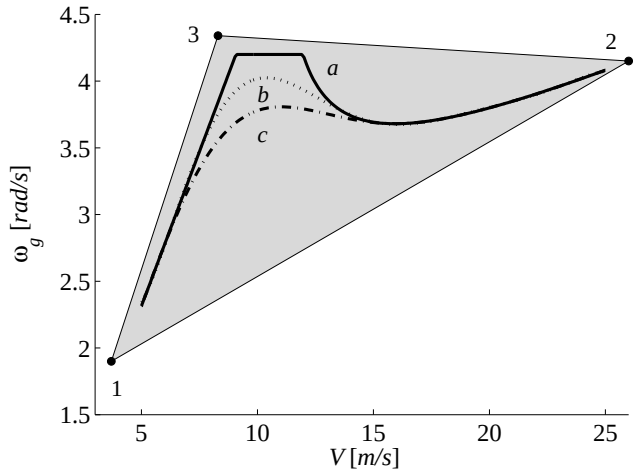

Figure 7. Possible parameter trajectories and polytope Θ.

Fig. 7 shows the selected polytope Θ on the parameter space $\omega - V$ and the operating points of Fig. 4 (curve a in Fig. 7). It is possible to synthesize the controller over the trajectory a, however synthesis in the convex region Θ is considerably simpler, and other trajectories as b and c can also be tracked (**?**).

It is interesting to observe that LPV gain scheduling approach assures stability and performance for all closed loop systems in Θ. Therefore, if the magnitude of the mentioned parameter errors are such that the resulting closed loop systems remain within Θ, then the stability and performance are maintained.

5.2 Controller design

In this subsection, Novak's approach (**?**) is conceptually improved in a more robust context. More specifically, the controller K and the gain k_β in Fig. 5 are replaced by a LPV controller. Then, using the concepts summarized in Section 2, a strategy that fulfills the control objectives in every point within the polytope Θ is obtained.

The setup of the LPV gain scheduling synthesis problem is similar to one of $\mathcal{H}_\infty$ optimal control. The plant is augmented with weighting functions that introduce the objectives into the problem. Fig. 8 shows a block diagram of the augmented plant with the following functions

$$M(s) = \frac{10s+1}{s}, \tag{32}$$

$$W_e(s) = \frac{0.5}{10s+1}, \tag{33}$$

$$W_q(s) = \frac{s}{20(s+10)}, \tag{34}$$

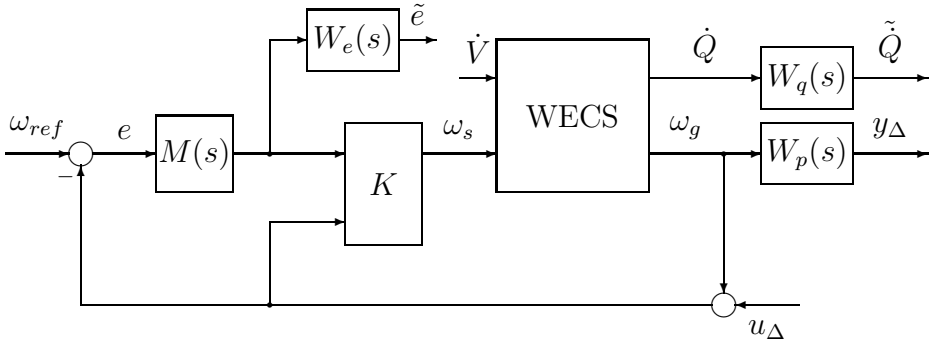

Figure 8. Block diagram of the augmented plant.

$$W_p(s) = \frac{5s}{s + 2500}. \tag{35}$$

The weighting functions $M(s)$ and $W_e(s)$ consider the generation objective, that is the tracking of speed reference ω_{ref}. $M(s)W_e(s)$ forces the steady state error to zero, allowing a larger error at high frequencies. Note that good tracking at high frequencies is not recommended because it increases the dynamic load. On the other hand, the weighting function $W_q(s)$ stresses the frequency range near the resonant modes to increment damping. Finally, the function $W_p(s)$ considers the high frequency uncertainty where the goal is to restrict the closed loop bandwidth.

Once the problem setup has been completed, the controller is obtained by solving the set of LMIs indicated in Section 2. The eigenvalues of the closed loop matrices A_{cl_i} are confined to the region $\mathrm{Re}(s) \geq -10^4$, avoiding the excessive fast modes of the controller that may appear in this synthesis procedure. Besides, a parameter dependent scaling with $\mathbf{diag}(s_1, s_2, s_3)$ structure is considered, given that the objectives consist in minimizing the infinite norm of the operators $u_\Delta \to y_\Delta$, $\omega_{ref} \to e$ and $\dot{V} \to \dot{Q}$.

The performance of the proposed LPV controller will be compared with a fixed $\mathcal{H}_\infty$ controller. For the $\mathcal{H}_\infty$ design, the parameter vector is considered uncertain, and the affine LPV model (29) is converted to the LFT form (see, for example, **?**). The augmented plant and the weighting functions are the same than the ones of LPV case.

Fig. 9 shows the simulation of the nonlinear closed loop system when a wind speed test signal is applied, and the speed reference is computed according to trajectory a in Fig. 7. The selected test signal covers the three operating regions with a rise time in agreement with the maximum bandwidth of the wind speed measurement. Although this signal is not real, the goal is to test the controller performance in an extremely demanding situation. In Fig. 9, the thin line corresponds to the system with the $\mathcal{H}_\infty$ controller and the thick line to the LPV controller. Notice that the latter presents better reference tracking than the former.

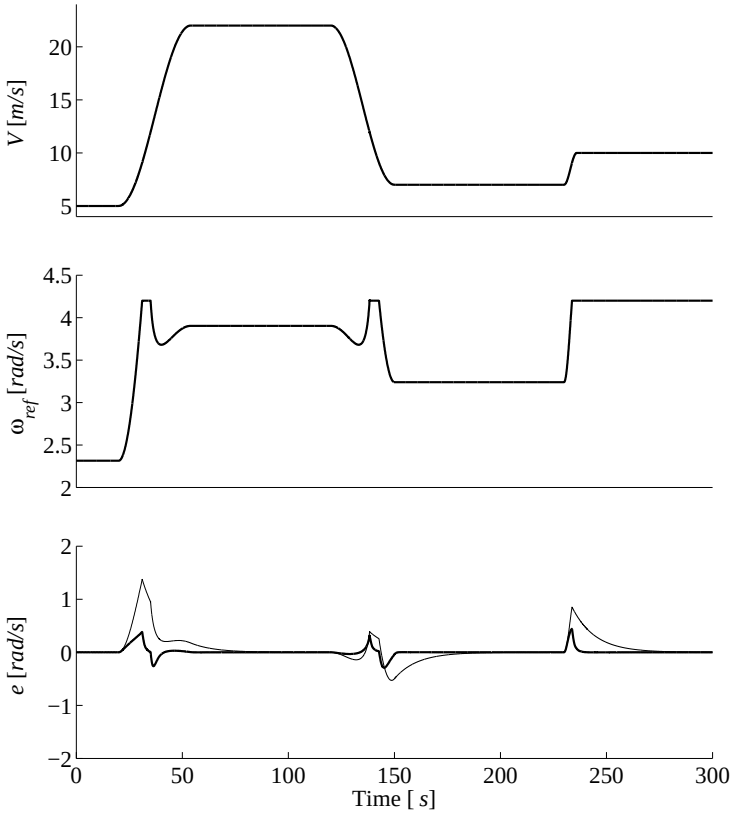

Figure 9. Closed loop simulations with $\mathcal{H}_\infty$ controller (thin line) and with LPV controller (thick line). 1-Wind speed test signal V, 2-turbine speed reference ω_{ref} according to trajectory a, 3-speed error $e = \omega_{ref} - \omega_g$.

Fig. 10 presents closed loop simulations using a realistic wind speed profile with mean $7.5m/s$. In this situation, the wind speed is in the optimal tracking region, and thus the speed reference is computed from $\lambda_{opt}V/R$ (3.5 rad/s, in this example). At this turbine speed, the cyclic disturbances of frequency $N\omega$ excite the resonant mode at 6.7 rad/s ($N = 2$ for the present example). In the top plot in Fig. 10, the thick and the dashed lines correspond to the measured wind speed V and the actual wind speed, respectively. In the other plots, the thick lines correspond to the system with the LPV controller while the thin ones are the responses with the $\mathcal{H}_\infty$ control. It can be observed that the magnitudes of the speed error and the torque oscillations are considerably smaller in the LPV case.

The smaller torque oscillation in the LPV case is in agreement with the frequency responses of the operator $V \to Q$, at fixed θ, presented in Fig. 11. Observe that while the LPV controller (thick line) reduces the resonant peak, the transfers $V \to Q$ corresponding to $\mathcal{H}_\infty$ control (thin line) and open loop (dotted line) are almost coincident.

Clearly, the LPV controller presents better tracking and more damping of

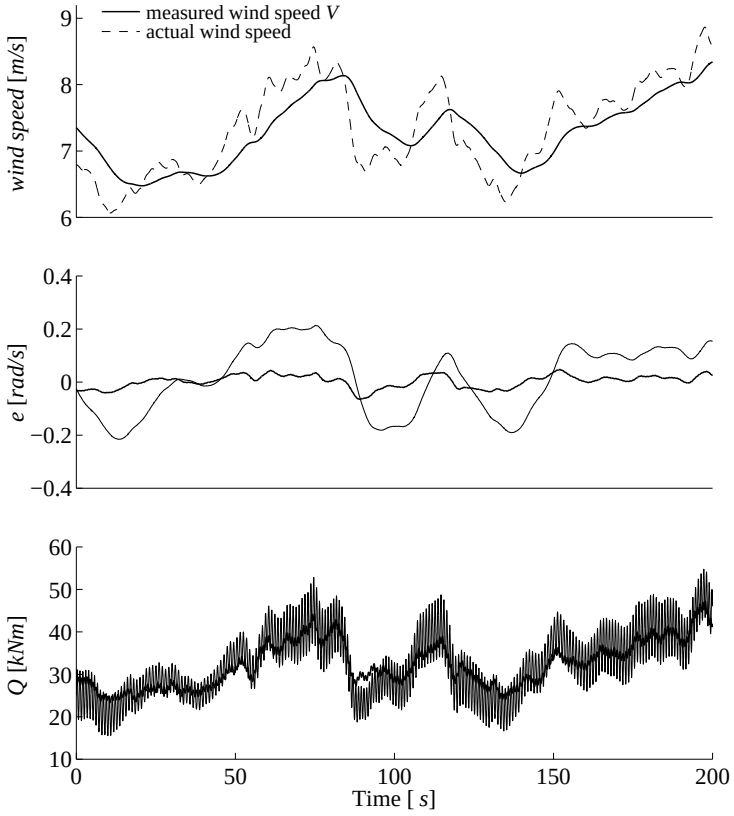

Figure 10. Closed loop simulations with $\mathcal{H}_\infty$ controller (thin line), and with LPV controller (thick line). 1-Wind speed, 2-speed error $e = \omega_{ref} - \omega_g$, 3-shaft torque Q.

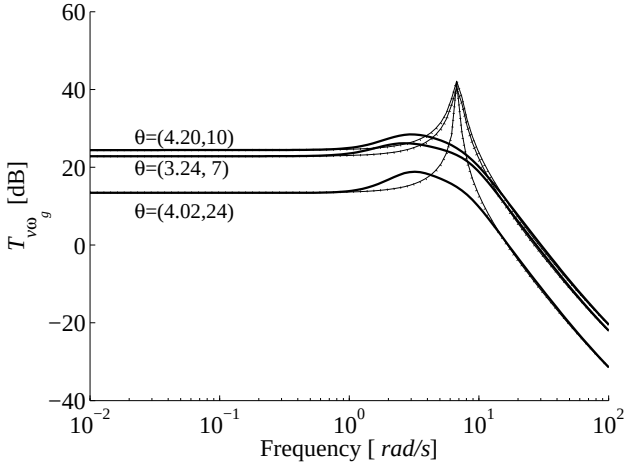

Figure 11. Bode plots of the operator $V \to Q$ evaluated at three fixed θ. (dotted line) Open loop system, (thin line) closed loop system with $\mathcal{H}_\infty$ controller and (thick line) closed loop system with LPV controller.

resonant modes because its ability to adapt itself to the wind conditions. Specially, this last objective is rather difficult to satisfy. Consequently, only the LPV controller, which is less conservative, is able to achieve a more considerable reduction of the oscillations with regard to the open loop system.

6 Conclusion

In this paper, a LPV gain scheduling strategy for variable-speed WECS has been proposed. This control achieves maximization of the conversion efficiency, safe operation and reduction of the torque oscillations whereas it considers high frequency uncertainty. In particular, the damping increment concept is used to improve the reduction of the torque oscillations.

Due to the nonlinear nature of variable-speed WECS and their wide operating range, controllers that are valid in all operating points are excessively conservative. Then, to obtain less conservative strategies is an important point in the variable-speed WECS control. In this sense, the proposed LPV control is very promising since it combines a design procedure similar to $\mathcal{H}_\infty$ control with the adaptability of gain scheduling. Equally important, it is the system formulation as a convex optimization problem with LMIs that allows the incorporation of additional constraints as pole clustering to simplify the implementation.

Acknowledgements

This work was supported by the Agencia Nacional para la Promoción Científica y Técnica ANPCyT, the Comisión de Investigaciones Científicas de la prov. de Buenos Aires CICpBA, the Consejo Nacional de Investigaciones Científicas y Técnicas CONICET and the Universidad Nacional de La Plata UNLP. The authors wish to thank Pablo Puleston for helpful comments.

A Appendix

Parameters corresponding to the $400kW$ WECS used in the simulations

$$
\begin{aligned}
N &= 2, \\
R &= 17.5m, \\
J_t &= 160Tm^2, \\
J_g &= 70Tm^2, \\
B_s &= 50Tm^2/s, \\
K_s &= 7500Tm^2/s^2.
\end{aligned}
$$